SCISPACE
formerly Typeset

Open access • Journal Article • DOI:10.1103/PHYSREVA.94.041802

Deterministic light focusing in space and time through multiple scattering media with a time-resolved transmission matrix approach — Source link

Mickael Mounaix, Hugo Defienne, Hugo Defienne, Sylvain Gigan

Institutions: PSL Research University, Princeton University

Published on: 17 Oct 2016 - Physical Review A (American Physical Society)

Topics: Ultrashort pulse, Coherent control, Spatial light modulator, Scattering and Matrix (mathematics)

Related papers:

- Measuring the transmission matrix in optics: an approach to the study and control of light propagation in disordered media.
- Focusing and compression of ultrashort pulses through scattering media
- Control of light transmission through opaque scattering media in space and time
- Spatiotemporal Coherent Control of Light through a Multiple Scattering Medium with the Multispectral Transmission Matrix.
- Spatio-temporal focusing of an ultrafast pulse through a multiply scattering medium.

Share this paper:

View more about this paper here: https://typeset.io/papers/deterministic-light-focusing-in-space-and-time-through-4kt58la8t6

PHYSICAL REVIEW A **94**, 041802(R) (2016)

Deterministic light focusing in space and time through multiple scattering media with a time-resolved transmission matrix approach

Mickael Mounaix,[1,*] Hugo Defienne,[1,2] and Sylvain Gigan[1]

[1]*Laboratoire Kastler Brossel, ENS-PSL Research University, CNRS, UPMC Sorbonne Universités, Collège de France, 24 rue Lhomond, 75005 Paris, France*

[2]*Department of Electrical Engineering, Princeton University, Princeton, New Jersey 08544, USA*

(Received 26 July 2016; published 17 October 2016)

We report a method to characterize the propagation of an ultrashort pulse of light through a multiple scattering medium by measuring its time-resolved transmission matrix. This method is based on the use of a spatial light modulator together with a coherent time-gated detection of the transmitted speckle field. Using this matrix, we demonstrate the focusing of the scattered pulse at any arbitrary position in space and time after the medium. Our approach opens different perspectives for both fundamental studies and applications in imaging and coherent control in disordered media.

DOI: 10.1103/PhysRevA.94.041802

When coherent light propagates in a scattering medium, light exits the system under the form of a speckle pattern [1], the result of complex interference effects between all the scattered waves. All the information carried by the incoming light is scrambled in the transmitted field. Multiple scattering of light is then an adverse effect for most optical imaging applications [2]. This wave mixing process is certainly complex, but it is deterministic. In the last years, wave-front shaping techniques have exploited the deterministic nature of light scattering to control light propagation in scattering media, using spatial light modulators (SLMs). These techniques have demonstrated the control of coherent light propagating through a layer of paint or through multimode fibers using either an iterative optimization approach [3] or digital phase conjugation [4]. Wave-front shaping techniques have also been used to measure the monochromatic scattering matrix of a disordered medium [5]. This complex operator links any input field of the medium to its corresponding output field and can be used to focus light or to image through a disordered medium [5–7]. The matrix approach has been applied to many different systems, such as multimode fibers [8], and extended to different fields of optics, such as photoacoustics [9] or quantum optics [10].

Light propagation in a disordered system has also been investigated with low-coherence sources such as ultrashort pulse lasers. In this situation, light is mixed spatially but also stretched temporally during its propagation, and speckle patterns in space and time are generated at the output. Pulse recompression can be achieved via spectral shaping [11]. Counterintuitively, shaping only the spatial properties also enables spatiotemporal control owing to the spatiotemporal coupling performed by the medium, as demonstrated in acoustics [12] and in optics [13–17]. Other approaches based on the measurement of a time-resolved reflection matrix have also been proposed for focusing [18] or imaging [19,20] at a target depth inside a scattering medium. In this regime, the time-gated detection of backscattered photons aims at selecting a certain depth of the scattering sample, essentially by selecting ballistic photons, similarly to optical coherence tomography. However, when light propagates through a disordered medium with an optical thickness larger than several transport mean free paths, the diffusive regime is reached in transmission and no ballistic photons can be detected at the output. Recently, the deterministic control of an ultrashort pulse of light propagating through a multiple scattering medium has been achieved by measuring its multispectral transmission matrix (MSTM) [17,21]. This matrix characterizes light propagation for all the different wavelengths that compose the incoming pulse, and enables a deterministic spatiotemporal control of the scattered pulse at the output by exploiting the time-frequency duality. This approach has nevertheless an important practical drawback in that it requires full knowledge of the spectral information (i.e., the full measurement of the MSTM) to control accurately the output temporal speckle. Indeed, most of the information content of the MSTM is superfluous if one is only interested in manipulating light at a specific arrival time at the output.

In this Rapid Communication, we report an experimental measurement of a time-resolved transmission matrix (TRTM) of a scattering medium in the diffusive regime using a coherent time-gated detection. Unlike the MSTM approach, we demonstrate that a TRTM measured for a given single time enables efficient spatiotemporal focusing of the pulse at the chosen arrival time after the medium. Finally, we show that full knowledge of the TRTM enables shaping more sophisticated spatiotemporal profiles of the pulse at the output, such as pump-probe profiles.

Figure 1 sketches the experimental setup used to measure the TRTM of a scattering sample. A Ti:sapphire laser source (MaiTai, Spectra Physics) produces an ultrashort pulse centered around 800 nm with a duration of $\tau_0 \approx 110$ fs. The pulse is split between a reference and a control arm using a half-wave plate (HWP) and a polarizing beam splitter (PBS). In the control arm, a phase-only SLM (LCOS-SLM, Hamamatsu X10468) modulates the wave-front of the reflected pulse. The shaped pulse is then injected into a thick layer of ZnO nanoparticles (thickness of approximately 100 μm) using a microscope objective. Scattered light is collected on the other side of the medium using a microscope objective. Another

*mickael.mounaix@lkb.ens.fr

 ©2016 American Physical Society

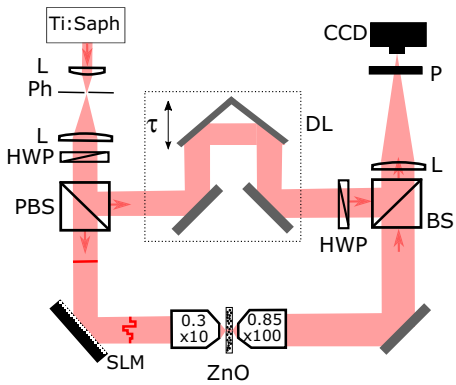

FIG. 1. Apparatus for measuring a time-resolved transmission matrix (TRTM) of a scattering medium. An ultrashort pulse of light generated by a Ti:sapphire laser [central frequency: 800 nm; $\tau_0 \approx$ 110 fs full width at half maximum (FWHM)] is split between a reference and a control path using a combination of a half-wave plate (HWP) and a polarizing beam splitter (PBS). In the control arm, the pulse is reflected by a SLM and injected into a sample of ZnO nanoparticles with a thickness of approximately 100 μm using a microscope objective. The scattered light is collected in transmission by another objective and interferes with the reference pulse onto a beam splitter (BS). The microscope objective together with the lens (L) image of the output surface of the scattering medium onto a charge-coupled device (CCD) camera. A polarizer (P) is used to select only one output polarization. The delay line (DL) inserted in the reference path controls the relative optical path delay between the reference and the scattered pulse. Ph: Pinhole.

microscope objective and a lens (L) are used to collect the scattered light and image the output surface of the medium onto a charge-coupled device (CCD) camera (Allied Vision, Manta G-046). Scattered and reference pulses are recombined before the camera using a beam splitter (BS) and one polarization is selected using a linear polarizer (P). A delay line (DL) inserted in the reference arm sets the relative optical path delay between the reference and the scattered pulses.

An ultrashort pulse of light propagating in a multiple scattering medium follows a large distribution of optical diffusive paths determined by the exact position of the scatterers. All these optical paths interfere at the output and generate a complex spatiotemporal speckle pattern [22]. Spatial and temporal features of the speckle are characterized respectively by the size of a speckle grain and by the traversal time of the medium, related to its dwell time τ_m. The dwell time depends only on the medium properties and refers to the duration during which the photons stay confined inside the medium, due to the broad path-length distribution in the sample because of multiple scattering events [23,24]. The spatiotemporal mixing performed by the medium is the equivalent of the spatiospectral coupling that has been investigated and reported in previous works [11,17,21]. One can define the spectral bandwidth of the medium $\Delta\lambda_m$ [17,21], which is the minimal difference in input wavelengths required to generate uncorrelated speckle patterns at the output, and which only depends on the medium properties. The spectral bandwidth is inversely proportional to the dwell time τ_m of the photons. Indeed, a pulse with a spectral bandwidth larger than the spectral bandwidth of the medium—or, in an equivalent way, a pulse with a temporal duration smaller than the dwell time of the medium—will experience spectral dispersion, or temporal broadening, during propagation.

Because a CCD camera is not fast enough to resolve the temporal structure of the pulse at the output, we estimate τ_m using the interferometric cross correlation (ICC) technique [25]. This linear pulse characterization technique enables one to retrieve the temporal envelope of the output speckle by interfering it with the Fourier-limited pulse of the reference arm. For this purpose, a set of intensity images is recorded with the CCD camera while the delay line of the reference arm is scanned. The signal measured at each pixel of the camera is then an interferogram produced by a combination of the output speckle measured at this specific pixel and the reference pulse. The temporal envelopes of the output pulses are finally retrieved from their interferograms by applying a low-pass filter. As presented in Fig. 2(a), the temporal structure of the output pulse averaged over 100 different speckle grains shows the expected exponential decay profile [17]. The dwell time is estimated

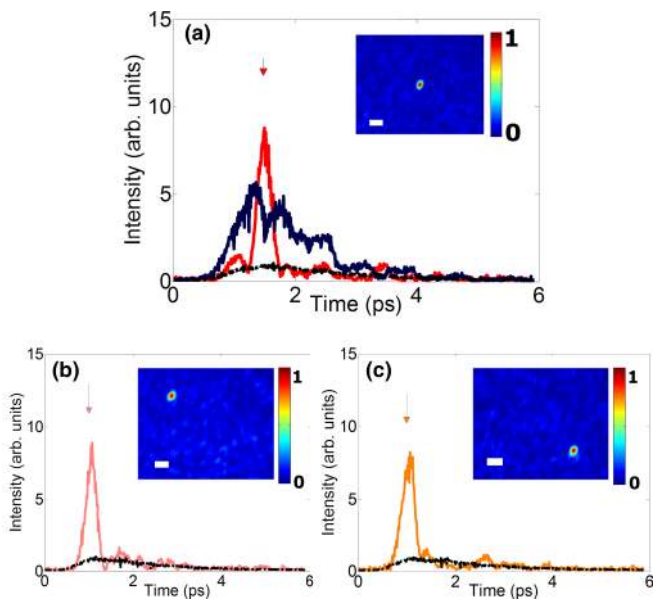

FIG. 2. Results of spatiotemporal focusing at a given output position and a given time by phase conjugating the time-resolved transmission matrix $H(t_a)$ measured at the arrival time $t_a = 1.6$ ps (denoted by the top arrows). (a) Temporal profiles recorded at the targeted spatial output position in cases of spatiotemporal focusing (red) and spatial-only focusing (blue line) processes. The spatial-only focusing process is performed by applying the phase-conjugation technique to a monochromatic transmission matrix measured at the central wavelength of the incoming pulse. The target position is visible on the CCD image in the inset. An average output temporal profile of the pulse (black line) is obtained by averaging temporal profiles over 100 different speckle grains at the output. The dwell time of the medium is evaluated from this averaged profile to be about $\tau_m \simeq 2$ ps. (b) and (c) show temporal profiles and the corresponding CCD camera images for spatiotemporal focusing processes performed at two different spatial positions using the same transmission matrix $H(t_a)$. The averaged temporal profiles are drawn in black. The scale bars on the CCD images in the inset correspond to 2 μm.

from the averaged profile to be about $\tau_m \simeq 2$ ps $\sim 20\tau_0$. The output pulse is therefore broadened on average by a factor $\simeq 20$ relative to the original pulse.

Owing to the linearity of the scattering process and the stability of the medium, the propagation of an optical pulse can be described by using a scattering matrix formalism. The optical field measured at a given arrival time t_a at the output is linked to the input field by the formula

$$E^{\text{out}}(t_a) = H(t_a)E^{\text{in}}, \tag{1}$$

where E^{in} is a complex vector containing the amplitude and phase values of the field for each input mode (i.e., a SLM pixel), $E^{\text{out}}(t_a)$ is a complex vector containing the amplitude and phase values of the field for each output mode (i.e., a CCD camera pixel) measured at a specific arrival time t_a, and $H(t_a)$ is the transmission matrix measured at t_a connecting inputs to outputs. A complete set of matrices $\{H(t_a)\}_{t_a}$ forms the full TRTM of the scattering medium.

Spatiotemporal focusing of the transmitted pulse is achieved first by measuring the time-resolved matrix $H(t_a)$. The matrix is measured column by column by recording the output fields for a set of N SLM patterns at the input. Each transmitted field is retrieved from intensity measurements on the CCD camera at the output using a phase-stepping holographic process, as in a monochromatic case [5]. However, in contrast with Ref. [5], the ultrashort reference pulse provides a time gating since the interference can only come from a time window given by the pulse duration. Furthermore, the targeted detection time t_a can be set by adjusting the delay line.

The pattern to be programmed on the SLM for focusing light in space and time is then calculated by using a phase-conjugation approach as in Ref. [5],

$$E^{\text{in}} = H^{\dagger}(t_a)E_x^{\text{target}}, \tag{2}$$

where $H^{\dagger}(t_a)$ is the conjugate transpose of $H(t_a)$ and E_x^{target} is a null vector with a coefficient 1 at the row corresponding to the targeted position x on the camera. Performing a digital phase conjugation [see Eq. (2)] corresponds to controlling the phases of the input modes, and then consequently the global phases of the speckle patterns they generate at the output. Thus we precisely set these speckles to interfere constructively at the targeted output mode [5]. Owing to the time gating due to the reference pulse during the matrix measurement, this constructive interference process occurs only for a specific arrival time. This operator acts precisely as a time-reversal operator for the arrival time t_a and light is focused both in space and time at the output [26].

The results of spatiotemporal focusing of a 110 fs pulse transmitted through a thick layer of paint using a set of $N = 256$ input modes are shown on Fig. 2. The time-resolved matrix $H(t_a)$ is measured at the arrival time $t_a = 1.6$ ps, as indicated by the top arrows. For a single time, the matrix measurement process takes about 2 min, this time being mostly limited by the refresh rate of the SLM. The SLM is then programmed using the phase-conjugation approach and the temporal profile of the output pulse at the targeted spatial position is reconstructed with an ICC measurement. As presented in Fig. 2(a), the temporal profile of the resulting focused pulse (red) shows a peak of intensity centered at t_a with a temporal width of 150 fs, close to the width of the Fourier-limited incoming pulse (110 fs). This pulse profile is compared to the temporal profile (blue) acquired using a spatial-only focusing process, which is achieved by phase conjugation of the monochromatic transmission matrix measured at the central wavelength of the pulse [17]. As expected, no temporal compression is observed in this case, but the intensity measured at the targeted pixel on the CCD camera remains more intense than the background [17]. By changing E^{target} in Eq. (2), the output pulse can be focused at any arbitrary output position. As presented in Figs. 2(b) and 2(c), the resulting temporal profiles for focusing at two different spatial positions show the same temporal compression at the arrival time $t_a = 1.6$ ps. As expected, the intensity enhancements observed on the CCD camera are also similar (insets).

Full spatiotemporal control of the pulse at the output requires the measurement of a larger set of time-resolved transmission matrices. In Fig. 3, seven transmission matrices have been recorded at seven different arrival times distributed between $t_1 = 1.6$ ps and $t_7 = 4.6$ ps. The time gap between two targeted arrival times $|t_i - t_j|$ is set larger than the time width of a temporal speckle grain, which corresponds also to

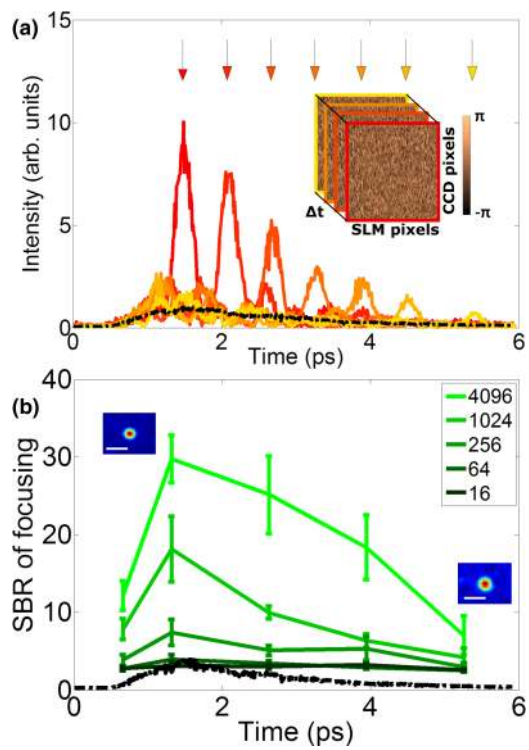

FIG. 3. Spatiotemporal control of light with a set of transmission matrices $\{H(t_a)\}_{t_a}$ measured at different arrival times. (a) Temporal profiles acquired using spatiotemporal focusing processes at the same output position and different arrival times (colored arrows). The spatially averaged speckle is used as a reference temporal profile (black curve). Phase components of the TRTM measured are drawn in the inset. (b) Signal-to-background ratio (SBR) measured on the CCD camera for different targeted arrival times and different numbers of modes controlled at the input. The SBR is the ratio of the intensity at the targeted pixel of the CCD camera over the mean intensity value of the full speckle image. The scale bar is 2 μm.

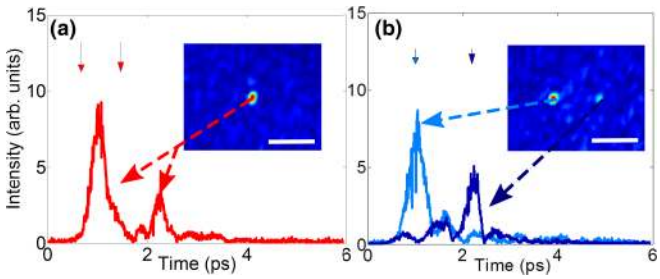

FIG. 4. Complex spatiotemporal shaping of the output pulse by exploiting the full TRTM. (a) Temporal profiles recorded using a spatiotemporal focusing process at one spatial position and two different arrival times $t_1 = 1$ ps and $t_2 = 2.2$ ps. The CCD image in the inset shows the position of the spatial target. (b) Temporal profiles recorded using a spatiotemporal focusing process at the same two different arrival times and at two different spatial positions, visible on the CCD image in the inset. The scale bar is 5 μm.

the time width of the initial input pulse [17], to ensure the matrices are well uncorrelated with each other. As presented in Fig. 3(a), each matrix of the set can be independently used to perform spatiotemporal focusing at different arrival times.

The efficiency of the spatiotemporal focusing process can be analyzed by measuring a signal-to-background ratio (SBR) on the CCD images recorded at the output. The SBR is the ratio of the intensity at the targeted pixel of the CCD camera over the mean intensity value of the full speckle image, integrated over the acquisition time of the camera. As shown in Fig. 3(b), SBR values depend both on the targeted arrival time and the number of modes controlled at the input. For a given arrival time, the SBR increases with the number of modes controlled, and for a fixed number of controlled modes, maximal values of SBR are always reached for the targeted arrival time that corresponds to the maximum of intensity in the averaged temporal profile. Besides, we observe that spatiotemporal focusing may be achieved even for a very long arrival time ($t_7 \approx 4.6$ ps) where the photon rate is very low, provided the number of modes controlled is sufficiently high. As the input light is broadband, the values of SBR measured in this experiment are much lower than the one observed in the monochromatic case [22], and also much lower than the peak-to-background intensity that would be obtained at the target time t_a.

The TRTM can also be used to shape more complex spatiotemporal profiles at the output. For example, spatiotemporal focusing at two different positions x_1 and x_2 and two different times t_1 and t_2 simultaneously is achieved by calculating the SLM pattern using a combination of the corresponding matrices $H(t_1)$ and $H(t_2)$,

$$E^{\text{in}} = H^{\dagger}(t_1)E_{x_1}^{\text{target}} + H^{\dagger}(t_2)E_{x_2}^{\text{target}}, \tag{3}$$

where $E_{x_1}^{\text{target}}$ ($E_{x_2}^{\text{target}}$) is a null vector containing a coefficient 1 at the line that corresponds to the position x_1 (x_2) of the camera. Figure 4(a) shows results of spatiotemporal focusing in the particular case of $x_1 = x_2$ with $t_1 = 1$ ps and $t_2 = 2.2$ ps. Logically, we observe that the intensity values of the two successive peaks are approximately half the intensities obtained for the same arrival times using simple spatiotemporal focusing processes presented in Fig. 3 with the same number of input modes ($N = 256$). Such a deterministic pump-probe-like pulse has an interesting potential for applications in light-matter interactions in scattering media [27]. Results obtained by generalizing this process to the case $x_1 \neq x_2$ are shown in Fig. 4(b). The output speckle is now focused simultaneously at two different times ($t_1 = 1$ ps and $t_2 = 2.2$ ps, visible on temporal profiles) and at two different speckle grains (visible on the CCD image in the inset).

It is interesting to compare the TRTM approach demonstrated here to the multispectral approach of Ref. [17]. Although the MSTM and the TRTM contain in principle the same information, the most adapted depends on the experiment to be performed. While the MSTM could address the spectral dispersion by a phase control on all the spectral components of the output pulse, the TRTM enables a direct temporal refocusing by adjusting the optical paths with the same arrival time at the output of the medium. Clearly, recompressing the pulse at the output at a given time is much easier and faster when using the TRTM, as it requires measuring a single time-resolved transmission matrix, rather than measuring the MSTM for all the spectral components, then recombining them accordingly. Nonetheless, narrow-band focusing as well as more refined pulse control, in the phase and in amplitude, of the output pulse is more straightforward when using the MSTM.

In conclusion, we have demonstrated deterministic spatiotemporal focusing of an output pulse after propagation through a disordered medium, with a single measurement of a transmission matrix of the medium at a given arrival time. Combining several scattering matrices from the full TRTM enables spatiotemporal focusing at different times using a single SLM. This approach, complementary to the other spectral or temporal approaches to light control in complex media, could enable potential applications in multiphotonic imaging and light-matter interactions in disordered media.

The authors would like to thank Thomas Chaigne, Samuel Grésillon, and Ori Katz for fruitful discussions. This work was funded by the European Research Council (Grant No. 278025). S.G. acknowledges support as a member of the Institut Universitaire de France.

[1] J. W. Goodman, J. Opt. Soc. Am. A **66**, 1145 (1976).
[2] V. Ntziachristos, Nat. Methods **7**, 603 (2010).
[3] I. M. Vellekoop and A. P. Mosk, Opt. Lett. **32**, 2309 (2007).
[4] I. N. Papadopoulos, S. Farahi, C. Moser, and D. Psaltis, Opt. Express **20**, 10583 (2012).
[5] S. M. Popoff, G. Lerosey, R. Carminati, M. Fink, A. C. Boccara, and S. Gigan, Phys. Rev. Lett. **104**, 100601 (2010).
[6] S. M. Popoff, G. Lerosey, M. Fink, A. C. Boccara, and S. Gigan, Nat. Commun. **1**, 81 (2010).

[7] Y. Choi, T. D. Yang, C. Fang-Yen, P. Kang, K. J. Lee, R. R. Dasari, M. S. Feld, and W. Choi, Phys. Rev. Lett. **107**, 023902 (2011).

[8] J. Carpenter, B. J. Eggleton, and J. Schröder, Opt. Express **22**, 96 (2014).

[9] T. Chaigne, O. Katz, A. C. Boccara, M. Fink, E. Bossy, and S. Gigan, Nat. Photonics **8**, 58 (2014).

[10] H. Defienne, M. Barbieri, I. A. Walmsley, B. J. Smith, and S. Gigan, Sci. Adv. **2**, e1501054 (2016).

[11] D. J. McCabe, A. Tajalli, D. R. Austin, P. Bondareff, I. A. Walmsley, S. Gigan, and B. Chatel, Nat. Commun. **2**, 447 (2011).

[12] F. Lemoult, G. Lerosey, J. de Rosny, and M. Fink, Phys. Rev. Lett. **103**, 173902 (2009).

[13] J. Aulbach, B. Gjonaj, P. M. Johnson, A. P. Mosk, and A. Lagendijk, Phys. Rev. Lett. **106**, 103901 (2011).

[14] O. Katz, E. Small, Y. Bromberg, and Y. Silberberg, Nat. Photonics **5**, 372 (2011).

[15] E. E. Morales-Delgado, S. Farahi, I. N. Papadopoulos, D. Psaltis, and C. Moser, Opt. Express **23**, 9109 (2015).

[16] H. P. Paudel, C. Stockbridge, J. Mertz, and T. Bifano, Opt. Express **21**, 17299 (2013).

[17] M. Mounaix, D. Andreoli, H. Defienne, G. Volpe, O. Katz, S. Grésillon, and S. Gigan, Phys. Rev. Lett. **116**, 253901 (2016).

[18] Y. Choi, T. R. Hillman, W. Choi, N. Lue, R. R. Dasari, P. T. C. So, W. Choi, and Z. Yaqoob, Phys. Rev. Lett. **111**, 243901 (2013).

[19] S. Kang, S. Jeong, W. Choi, H. Ko, T. D. Yang, J. H. Joo, J.-S. Lee, Y.-S. Lim, Q.-H. Park, and W. Choi, Nat. Photonics **9**, 253 (2015).

[20] A. Badon, D. Li, G. Lerosey, A. C. Boccara, M. Fink, and A. Aubry, arXiv:1510.08613.

[21] D. Andreoli, G. Volpe, S. Popoff, O. Katz, S. Grésillon, and S. Gigan, Sci. Rep. **5**, 10347 (2015).

[22] A. P. Mosk, A. Lagendijk, G. Lerosey, and M. Fink, Nat. Photonics **6**, 283 (2012).

[23] N. Curry, P. Bondareff, M. Leclercq, N. F. van Hulst, R. Sapienza, S. Gigan, and S. Grésillon, Opt. Lett. **36**, 3332 (2011).

[24] M. S. Patterson, B. Chance, and B. C. Wilson, Appl. Opt. **28**, 2331 (1989).

[25] A. Monmayrant, S. Weber, and B. Chatel, J. Phys. B **43**, 103001 (2010).

[26] A. Derode, P. Roux, and M. Fink, Phys. Rev. Lett. **75**, 4206 (1995).

[27] R. Sapienza, P. Bondareff, R. Pierrat, B. Habert, R. Carminati, and N. Van Hulst, Phys. Rev. Lett. **106**, 163902 (2011).